Mean magnitude variations of earthquakes as a function of depth: Different crustal stress distribution depending on tectonic setting

M. Wyss, F. Pacchiani, Anne Deschamps, G. Patau

Mean magnitude variations of earthquakes as a function of depth: Different crustal stress distribution depending on tectonic setting

M. Wyss,[1] F. Pacchiani,[2] A. Deschamps,[3] and G. Patau[4]

Received 20 June 2007; revised 7 September 2007; accepted 10 December 2007; published 15 January 2008.

[1] The mean magnitude of earthquakes in the Gulf of Corinth is found to increase strongly with depth (*b*-value decreases), whereas the dip of fault planes decreases. The *b*-value difference of 0.25, between shallow and deep earthquake distributions, is based on about 7,000 events and therefore is statistically highly significant. The same is true in California, but opposite patterns are observed in southern Iceland and in western Nagano, Japan. Because large mean magnitudes (low *b*-values) are indicative of relatively high stress levels, we propose that in the detachment layer at about 9 ± 2 km depth, earthquakes are generated at higher stresses than in the shallower parts of the crust. The correlation of low *b*-values with low faulting dips can be taken as line of evidence that low *b*-values map high stress regimes. **Citation:** Wyss, M., F. Pacchiani, A. Deschamps, and G. Patau (2008), Mean magnitude variations of earthquakes as a function of depth: Different crustal stress distribution depending on tectonic setting, *Geophys. Res. Lett.*, *35*, L01307, doi:10.1029/2007GL031057.

1. Introduction

[2] We map the local mean magnitude of earthquakes, $\overline{M}$, using the *b*-value, by equation (1) [*Aki*, 1965]

$$b = \frac{1}{2.3\left(\overline{M} - M_{\min}\right)}, \tag{1}$$

where $M_{\min}$ is the minimum magnitude in the local data and b is the slope of the linear fit to the frequency-magnitude distribution, FMD,

$$\log N = a - bM, \tag{2}$$

where N is the cumulative number of events and a is a constant that measures the seismicity rate.

[3] We discuss *b*-values instead of $\overline{M}$ to compare the distribution of $\overline{M}$ in data sets from several seismograph networks that work at different resolutions, i.e. different $M_{\min}$. Thus, comparisons of *b*-values can be easily understood, whereas values for $\overline{M}$ may be meaningless for the reader.

[4] $\overline{M}$ is proportional to the ambient stress in the local seismogenic volume (and by equation (1), b is inversely proportional to stress). *Scholz* [1968] has shown this in the laboratory for microfractures and has proposed a model explaining this phenomenon. The evidence that local *b*-values of earthquake distributions are inversely proportional to the ambient stress is the following: (1) *b*-values of the earthquakes triggered by pumping of fluids into the crust at Denver tracked the volume of liquid injected [*Wyss*, 1973]. (2) In underground mines, *b*-values were found to be inversely dependent on the stress level [*Urbancic et al.*, 1992]. (3) Known asperities along the San Andreas fault show low *b*-values [*Schorlemmer et al.*, 2004; *Wiemer and Wyss*, 1997]. (4) Increases of *b*-values that correlate with magmatic intrusions are best explained by increases of pore pressure [*Wiemer et al.*, 1998]. (5) High, medium and low *b*-values correlate worldwide with normal, strike-slip and thrust faulting, respectively [*Schorlemmer et al.*, 2005].

[5] To identify differences in stress level, we investigate differences in *b*-values, presenting the newly discovered decrease of *b*-values (increase of $\overline{M}$) with depth in the western Gulf of Corinth and comparing this pattern with patterns observed in Iceland, California and Japan.

2. Data

[6] The French national project GDR-Corinthe and the international projects CORSEIS and 3HAZ (crl.ens.fr/metadot) have operated a 12-station seismograph network since 2001 in the western Gulf of Corinth [*Lyon-Caen et al.*, 2004]. The stations are typically positioned 5 km apart.

[7] We mapped *Mc*, using the best combination method in zmap [*Wiemer*, 2001], starting with a large area, reducing it in steps. For each volume, we also calculated *Mc* as a function of time. Before selecting the final volume for analysis, we mapped *Mc* in cross section. In addition, we plotted the ratio of events recorded during nighttime to those recorded during daytime. These latter plots were helpful in verifying that for small *Mmin*, fewer events were reported during the day than during the night. An *Mc* = 1.3 leads to the best compromise for selecting the extent of good quality data in space and time and it leads to constant reporting during nighttime and daytime. Mapping *Mc*, we defined an area of about 25 km in diameter, centered on the network, that is complete at *M* = 1.3 out to the edges and to a depth of 15 km. At the center of this area, *Mc* is 1.1, and the ratio of nighttime to daytime events is nearly constant. Estimating *Mc* as a function of time revealed that the network experienced a period of buildup, during which resolution was poor. After the date of 2001.3, *Mc* was stable at 1.3. A search for explosions yielded none.

[1]World Agency of Planetary Monitoring and Earthquake Risk Reduction, Geneva, Switzerland.
[2]Laboratoire de Géologie, Ecole Normale Supérieure, Paris, France.
[3]Geosciences Azur, Université of Nice Sophia Antipolis, Centre National de la Recherche Scientifique/Pierre and Marie Curie University/Institut de Recherche pour le Développement, Valbonne, France.
[4]Département de Sismologie, Institut de Physique du Globe Paris, Paris, France.

0094-8276/08/2007GL031057$05.00

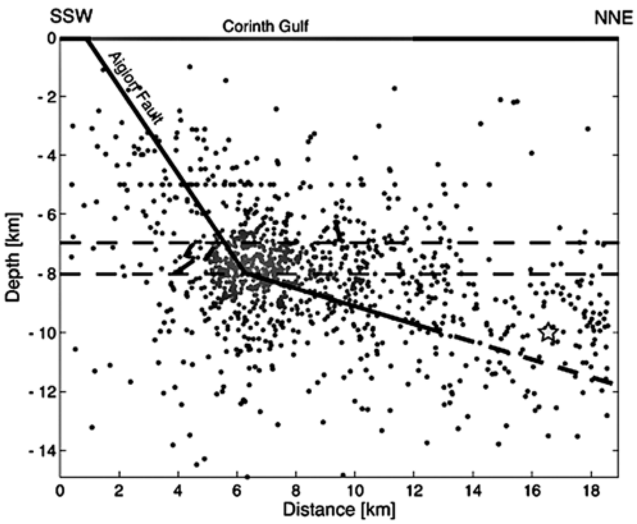

Figure 1. Cross section, 10 km wide, across the Corinth Gulf showing the best located hypocenters of earthquakes with $M \geq 1.3$, recorded between 2001.3 and 2006.2. The black lines schematically depict the fault structure inferred from the geometrical analysis of relocated multiplets. The dotted line represents the transition zone between high and low angle dipping multipelts. The star marks the hypocenter of the M6.2 Aigion earthquake, of 15 June 1995. The data including all events with $M \geq 1.1$ contain 5.5 times more earthquakes.

[8] We performed the analysis that follows using three catalogs, all for the period 2001.3 to 2006.2. For the most general analysis, we used events with $M \geq 1.1$, located down to a depth of 20 km (16,303 events), for a more restricted analysis, we used those with $M \geq 1.3$ and located at depths of less than 15 km (7,102 events). Finally, the analysis was repeated using only earthquakes with high quality locations, defined as events, which were located with at least three P-wave and three S-wave phases, had an rms less than 0.4 sec and absolute standard errors less than 2 km in x, y, z. In the data set of high quality locations, the minimum magnitude of completeness was elevated to Mc = 1.4. The number of events whose magnitude is equal to and larger than M1.4 was 2,155 (when $M \geq 1.3$ were included the number of events was 3,090). All data sets, with all aforementioned selections of Mc, yielded the same results, overall, with some details differing by small amounts. During the period covered, the largest earthquake had M = 3.8. The best located hypocenters used for b-value analysis and specified above are shown in Figure 1.

[9] The data used for comparison with the results from the Gulf of Corinth are the following. For southern Iceland, the catalog covering the volume containing the main shocks of M6 in 2000 and described in detail by *Wyss and Stefansson* [2006] was used. For Parkfield, the special high-accuracy catalog analyzed by *Wyss et al.* [2004] was used. For the Tokai-Kanto area, the catalog previously analyzed by *Wyss and Matsumura* [2002, 2005] was employed. In that catalog, the b-value increases with depth in the over-all data, however, details of the pattern vary as a function of location. Here we selected a subset of the data from western Nagano that shows the increase of b with depth most clearly. For each case, the homogeneity of reporting had been reviewed by the respective authors. The errors in depth estimates are less than 1.5 km in these catalogs.

3. Results

[10] Although the b-values are heterogeneous, varying between about 1 and 2.2 on a scale of approximately 2 km, they are predominantly high in the shallow layers and low in the deeper layers (Figure 2). We estimated the statistical significance of the difference of b between shallow and deep parts, using *Utsu*'s [1992] test. The difference was significant at divisions at any depth between 5.5 and 10 km, but there is a clear contrast between cuts above and below 7 km. When cutting above 7 km, the probability that the two samples come from the same population ranges from 10^{-3} to $7\ 10^{-3}$, whereas for cuts below 7 km the probabilities range from $2\ 10^{-5}$ to $2\ 10^{-4}$. The lowest value is reached at a cutting depth of 9 km. Thus, we conclude that the b-value decreases somewhat gradually with depth (Figure 3a), and the contrast between shallow and deep parts is expressed most strongly, if one cuts at 9 ± 1 km depth.

[11] For plotting the maps, samples were taken with N = 100 events at nodes of grids with a separation of 1 km. For the cross section, the node separation was the same and samples of N = 200 were used. In each sample, the minimum magnitude of completeness was automatically re-evaluated before estimating b. For samples where fewer than 50 events (80 events alternatively) were available for the determination of b (considering the local Mc and discarding events with $M < Mc$), the calculation was not performed. The analysis was also carried out, using constant radii of sizes that yielded approximately 100 to 200 events per sample (r = 2, 2.5 and 3 km, respectively). The visual appearance of the maps and cross sections was the same using the varied selection criteria.

[12] The average b-value as a function of depth in the Gulf of Corinth (Figure 3a) decreases from about 1.6 to a minimum of 1.2 at 10 km. Thus, at a depth of 8 to 12 km, proportionally more medium size earthquakes are produced than at other depths. This pattern is similar to the increase of mean magnitude (decrease of b) with depth found in California, for which area, *Gerstenberger et al.* [2001] performed a detailed analysis. Here, we confirm the previous results for California with a different data set that shows a decrease of b with depth near Parkfield, where a catalog with highly precise hypocenters exists (Figure 3c).

[13] In southern Iceland, the pattern is reversed: at depths shallower than 5 km b = 0.6, whereas b = 0.9 below 7 km depth (Figure 3b). The data shown in Figure 3b are the aftershocks of the two M6.6 main shocks of 2000. This data set covers a different period than the data used by *Wyss and Stefansson* [2006], who had previously also shown that b increases with depth in southern Iceland. *Wyss and Matsumura* [2002] have shown that the b-values increase with depth in the Tokai-Kanto, Japan, area. Similar to Gerstenberger's findings in California, the pattern in Japan is not everywhere the same. In Figure 3d, we show an example from western Nagano where the average b increases gradually with depth from 0.6 to 1.3.

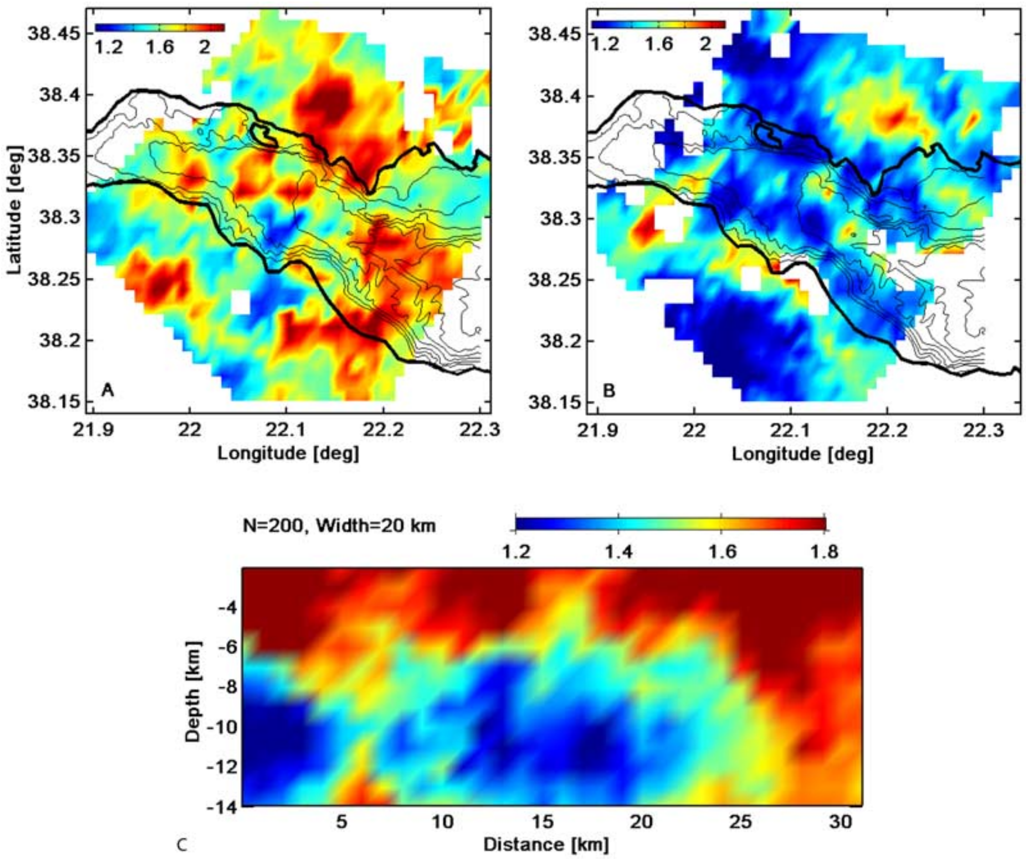

Figure 2. Maps of *b*-value in volumes with N = 100 events (a) above and (b) below 8 km. (c) Cross section from point 38.37N/21.95E to point 38.22N/22.25E, 20 km wide, showing *b* in volumes with N = 200 events. Coastlines are shown as solid black lines, fine lines demark the bathymetry. The catalog used included all events with $M \geq 1.1$. The shape of the sampling volumes was a cylinder with fixed height and varying radii.

[14] In order to verify that the differences are statistically significant, and to present the appearance of the frequency magnitude distribution (FMD) we compared the average FMD plots of shallow events with deeper ones for each area (Figure 4). These difference are judged highly significant by *Utsu*'s [1992] test, which we performed for a number of depth cuts. Given that the differences in *b* are typically 0.3 units and the numbers of events in each sample exceed 1,000, the probability that the compared samples come from the same population is invariably below 10^{-3}.

4. Discussion

[15] The tectonic process that generates earthquakes in the Gulf of Corinth is rifting in a NE-SW direction. GPS measurements show an extension rate of about 1.5 cm/year [*Briole et al.*, 2000; *Bernard et al.*, 2006] that is modeled by near-horizontal slip along the detachment plane shown in Figure 1 at about 8 km depth [*Bernard et al.*, 2006].

[16] In Iceland, the overall regime is also one of rifting, but in the southern Iceland seismic zone, the major earthquakes occur along near-vertical, N-S trending strike-slip faults [*Einarsson*, 1991]. The number of earthquakes increases steadily as a function of depth and drop abruptly below 10 km.

[17] In western Nagano, Japan, the faulting in the shallow crust takes place primarily as strike-slip on near-vertical planes in response to the EW compression due to underthrusting of the oceanic plates located east of Japan. Here the seismicity continues to depths greater than shown for comparison. The activity peaks at 10 km depth.

[18] Along the strike-slip fault segment at Parkfield, most earthquakes occur near 4 km depth, with minor peaks of activity at 7 and 9 km. Here, as in all of the data sets, the data from the mapped asperities and creeping sections were mixed for the overall analysis performed as a function of depth. Previously, *Gerstenberger et al.* [2001], using the USGS data, found that *b* decreased with depth in general, but not everywhere. Similar heterogeneities were found in all the data sets analyzed. In Figures 1–4 we present the prevalent trends. *Gerstenberger et al.* [2001] interpreted their observation as due to the increase of confining stress with depth.

[19] We propose that a similar mechanism of elevated stress is at work in the Gulf of Corinth leading to an increase of $\overline{M}$ with depth to 10 km (Figure 3a). *Pacchiani* [2006] relocated multiplets with high accuracy and was able to map the geometries of the fault planes on which the events occurred. He found that above 8 km depth the dips of the fault planes were relatively steep (60° on average) and below 8 km their dip was shallower (30° on average) (Figure 1). Thus, the overburden tends to clamp shut the faults at depth greater than 8 km and hence elevated shear stress is required

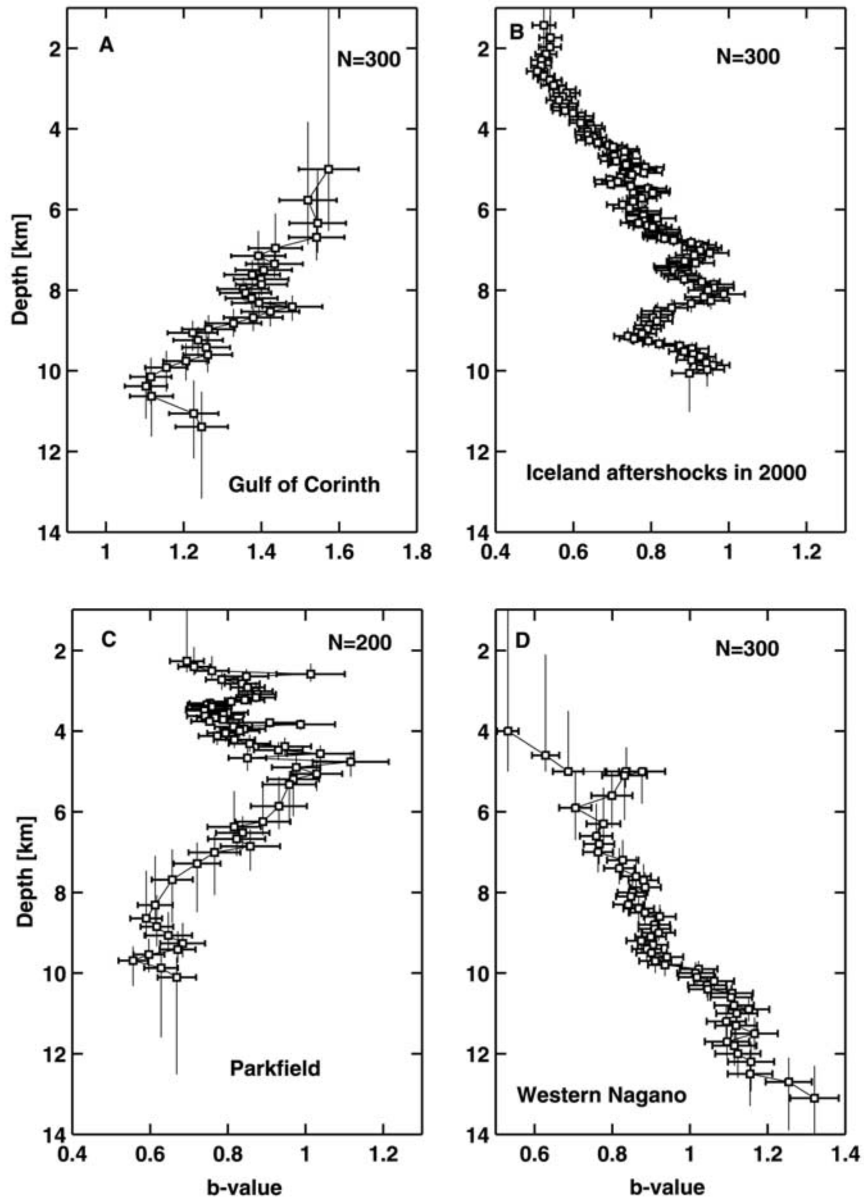

Figure 3. The *b*-values as a function of depth in overlapping samples of N events. For the Gulf of Corinth, only events with high quality hypocenter estimates and $M \geq 1.4$ were used. Error bars are calculated according to *Shi and Bolt* [1982]. The error bars do not overlap, and thus confirm the statistical significance of the difference between samples, elsewhere in this work estimated by the method of *Utsu* [1992].

to rupture these low angle faults, especially the detachment fault modeled by *Bernard et al.* [2006].

[20] At the very bottom of the seismicity in the Gulf of Corinth, the *b*-values increase (Figure 3a), suggesting that at the lower limit of the seismogenic layer faulting may occur under reduced stresses. This may be interpreted as due to elevated temperatures at the transition from brittle to ductile crust, which may allow faulting at reduced stresses.

[21] Our conceptual model for explaining the distribution of seismicity and mean magnitude with depth is as follows:

[22] 1. There are no earthquakes in the top few kilometers of the crust in any of the areas studied and *Labaume et al.* [2004] demonstrate extensive fluid processes in and around the fault planes in the Corinth rift at 1 to 2 km depth. We interpret this to mean that at shallow depths low normal stresses and pore pressures preclude build up of stress to the point of rupture by earthquakes. Deformation presumably takes place a-seismically [*Bernard et al.*, 2006].

[23] 2. The maxima of mean magnitude, demonstrated here to occur between 8 and 11 km depth beneath the Gulf of Corinth, suggests that stresses are concentrated there and main asperities from which main shocks are likely to emanate, are located at these depths. This agrees with relocations of hypocenters of the larger earthquakes in the Corinth rift by waveform modeling. For the M6.9 earthquake of 1981 in the eastern part of the rift, *Jackson et al.* [1982] found a hypocentral depth of 10 ± 2 km, for the M5.7 earthquake of 1992 (at the edge of the area studied here) the relocated depth was 7.4 ± 1 km [*Hatzfeld et al.*, 1996], and for the M6.2 earthquake that occurred in 1995 in

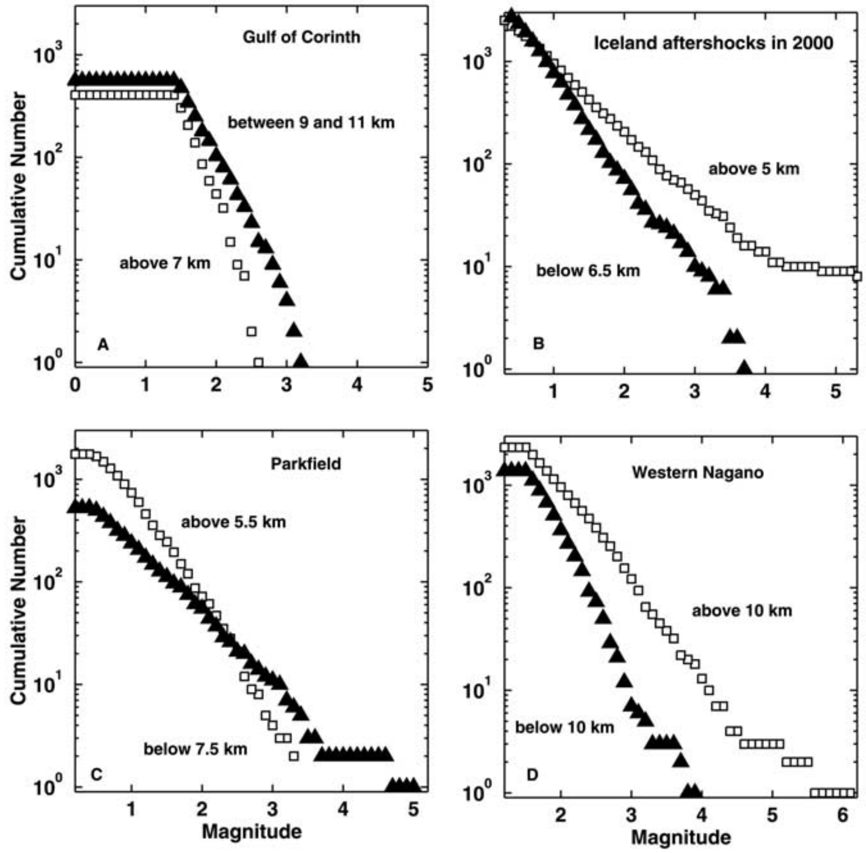

Figure 4. Cumulative numbers of earthquakes as a function of magnitude for the same areas as used in Figure 3. In each case, a shallow data set (open squares) is compared with a deeper one (solid triangles). For the Gulf of Corinth, $b = 1.55 \pm 0.06$ and $b = 1.16 \pm 0.04$ for shallow and deep samples, respectively, where the errors are calculated according to *Shi and Bolt* [1982].

the study area, *Bernard et al.* [1997] found a depth of 10 ± 3 km.

[24] 3. In the depth range of 4 to 7 km, seismicity exists, but is limited to smaller events than at depth and occurs along faults with steep dips at intermediate stress levels.

[25] The pattern of increasing *b*-values with depth observed in Iceland was interpreted as due to increasing pore pressure [*Wyss and Stefansson*, 2006] that allows faulting under lower stresses. This interpretation seemed attractive because various arguments had been put forth by other researchers that pore pressure increases with depth in southern Iceland [e.g., *Stefansson and Halldórsson*, 1988]. We do not know whether the same interpretation might be valid in Nagano. Currently, not enough areas have been examined in detail for establishing details of trends of mean magnitude with depth and along fault zones. Our results that reveal an increase of mean magnitude with depth in the Gulf of Corinth area, once again show that detailed mapping and analysis of *b*-values (or $\overline{M}$) have the potential of advancing our understanding of faulting processes and stress distribution in the crust.

[26] We conclude that the increased mean magnitude of earthquakes at depths of 8 to 10 km is further evidence that main shocks are generally expected to emanate from these depths in the Gulf of Corinth, and not from shallower layers. The evidence presented here, that low *b*-values (large $\overline{M}$) correlate with low dip angle of the fault planes, can be taken as another line of evidence that supports the hypothesis that low *b*-values map high stress regimes.

[27] **Acknowledgments.** We thank H. Lyon-Caen for providing the seismicity catalogs and S. Wiemer for his software zmap for analysis. We thank anonymous reviewers for helpful comments. This research was supported by the E.C. project 3HAZ-Corinth (contract GOCE 004043).

References

Aki, K. (1965), Maximum likelihood estimate of b in the formula log N = a − b M and its confidence limits, *Bull. Earthquake Res. Inst. Univ. Tokyo*, *43*, 237–239.

Bernard, P., et al. (1997), The Ms = 6.2, June 15, 1995 Aigion earthquake (Greece): Evidence of low angle normal faulting in the Corinth Rift, *J. Seismol.*, *1*, 131–151.

Bernard, P., et al. (2006), Seismicity, deformation and seismic hazard in the western rift of Corinth: New insights from the Corinth Rift Laboratory (CRL), *Tectonophysics*, *426*, 7–30.

Briole, P., A. Rigo, H. Lyon-Caen, R. G. Ruegg, K. Papazissi, C. Mitsakaki, A. Balodimou, G. Veis, D. Hatzfeld, and A. Deschamps (2000), Active deformation of the Corinth Rift, Greece: Results from repeated Global Positionning System surveys between 1990 and 1995, *J. Geophys. Res.*, *105*, 25,605–625,625.

Einarsson, P. (1991), Earthquakes and present-day tectonism in Iceland, *Tectonophysics*, *189*, 261–279.

Gerstenberger, M., S. Wiemer, and D. Giardini (2001), A systematic test of the hypothesis that the *b* value varies with depth in California, *Geophys. Res. Lett.*, *28*, 57–60.

Hatzfeld, D., et al. (1996), The Galaxidi earthquake of 18 November 1992: A possible asperity within the normal fault system of the Gulf of Corinth (Greece), *Bull. Seismol. Soc. Am.*, *86*, 1987–1991.

Jackson, J. A., J. Gagnepain, H. Houseman, G. C. P. King, P. Papadimitriou, C. Soufleris, and J. Virieux (1982), Seismicity, normal faulting, and the

geomorphological development of the Gulf of Corinth (Greece): The Corinth earthquakes of February and March 1981, *Earth Planet. Sci. Lett.*, *57*, 377–397.
Labaume, P., E. Carrio-Schaffhauser, J. F. Gamond, and F. Renard (2004), Deformation mechanisms and fluid-driven mass transfers in the recent fault zones of the Corinth Rift (Greece), *C. R. Geosci.*, *336*, 375–383.
Lyon-Caen, H., P. Papadimitriou, A. Deschamps, P. Bernard, K. Makropoulos, F. Pacchiani, and G. Patau (2004), First results of the CRLN seismic array in the western Corinth Gulf: evidence for old fault reactivation, *C. R. Geosci.*, *336*, 343–351.
Pacchiani, F. (2006), Etude sismologique des failles normales actives du Rift de Corinthe, PhD thesis, 373 pp., Univ. Paris XI, Paris.
Scholz, C. H. (1968), The frequency-magnitude relation of microfracturing in rock and its relation to earthquakes, *Bull. Seismol. Soc. Am.*, *58*, 399–415.
Schorlemmer, D., S. Wiemer, and M. Wyss (2004), Earthquake statistics at Parkfield: 1. Stationarity of *b* values, *J. Geophys. Res.*, *109*, B12307, doi:10.1029/2004JB003234.
Schorlemmer, D., S. Wiemer, and M. Wyss (2005), Variations in earthquake-size distribution across different stress regimes, *Nature*, *437*, 539–542.
Shi, Y., and B. A. Bolt (1982), The standard error of the magnitude-frequency b value, *Bull. Seismol. Soc. Am.*, *72*, 1677–1687.
Stefansson, R., and P. Halldórsson (1988), Strain release and strain build-up in the South Iceland seismic zone, *Tectonophysics*, *155*, 267–276.
Urbancic, T. I., C. I. Trifu, J. M. Long, and R. P. Young (1992), Space-time correlations of b-values with stress release, *Pure Appl. Geophys.*, *139*, 449–462.
Utsu, T. (1992), On seismicity, in *Report of the Joint Research Institute for Statistical Mathematics*, pp. 139-157, Inst. for Stat. Math., Tokyo.
Wiemer, S. (2001), A software package to analyze seismicity: ZMAP, *Seismol. Res. Lett.*, *72*, 373–382.
Wiemer, S., and M. Wyss (1997), Mapping the frequency-magnitude distribution in asperities: An improved technique to calculate recurrence times?, *J. Geophys. Res.*, *102*, 15,115–15,128.
Wiemer, S., S. R. McNutt, and M. Wyss (1998), Temporal and three-dimensional spatial analysis of the frequency-magnitude distribution near Long Valley caldera, California, *Geophys. J. Int.*, *134*, 409–421.
Wyss, M. (1973), Towards a physical understanding of the earthquake frequency distribution, *Geophys. J. R. Astron. Soc.*, *31*, 341–359.
Wyss, M., and S. Matsumura (2002), Most likely locations of large earthquakes in the Kanto and Tokai areas, Japan, estimated based on local recurrence time, *Phys. Earth Planet. Inter.*, *131*, 173–184.
Wyss, M., and S. Matsumura (2005), Verification of our previous definition of preferred earthquake nucleation areas in Kanto-Tokai, Japan, *Tectonophysics*, *417*, 81–84.
Wyss, M., and R. Stefansson (2006), Nucleation points of recent main shocks in southern Iceland mapped by b-values, *Bull. Seismol. Soc. Am.*, *96*, 599–608.
Wyss, M., C. Sammis, R. Nadeau, and S. Wiemer (2004), Comparison between seismicity on creeping and locked patches of the San Andreas fault near Parkfield, California: fractal dimension and b-value, *Bull. Seismol. Soc. Am.*, *94*, 410–424.

A. Deschamps, Geosciences Azur, Université of Nice Sophia Antipolis, CNRS/UPMC/IRD, 250 rue Albert Einstein, 06560 Valbonne, France.

F. Pacchiani, Laboratoire de Géologie, Ecole Normale Supérieure, 45 rue d'Ulm, F-75230 Paris, France.

G. Patau, Département de Sismologie, Institut de Physique du Globe Paris, 4 place Jussieu, F-75252 Paris, France.

M. Wyss, World Agency of Planetary Monitoring and Earthquake Risk Reduction, 2 rue de Jargonnant, CH-1207 Geneva, Switzerland. (wapmerr@maxwyss.com)